

## Article

# Friction Sensitivity Test Experiment and Desensitization Mechanism of Nitrocellulose-Coated DNTF Explosive Crystals

Junming Yuan <sup>1,\*</sup>, Yue Qin <sup>1</sup>, Yan Liu <sup>1</sup>, Hu Sun <sup>1</sup>, Runsheng Huang <sup>1</sup>, Jing Wang <sup>1</sup>, Tao Han <sup>1</sup> and Ruiqiang Wu <sup>2</sup>

<sup>1</sup> School of Environment and Safety Engineering, North University of China, Taiyuan 030051, China; cysl080579@163.com (Y.Q.); 18635820488@163.com (Y.L.); sunhudyx@163.com (H.S.); huangrs1998@yeah.net (R.H.); sz202214083@st.nuc.edu.cn (J.W.); h3581305@163.com (T.H.)

<sup>2</sup> Shanxi North Xing'an Chemical Industry Co., Ltd., Taiyuan 030008, China; wrq245204@163.com

\* Correspondence: yuanjm@nuc.edu.cn

**Abstract:** In response to the problem of the high friction sensitivity of 3,4-bis(3-nitrofurazan-4-yl) furoxan (DNTF) in solid propellants, the inherent component of solid propellants, nitrocellulose (NC), was used to coat DNTF explosives via the water suspension method. The coated samples were characterized by scanning electron microscopy (SEM) and friction sensitivity tests at a fixed 66° swing angle, and molecular dynamics calculations were performed to study the friction sensitivity and desensitization mechanism of NC-based DNTF coatings. The results show that NC, when used as a coating layer, can form a white gel on the surface of DNTF crystals, which can effectively reduce the friction sensitivity of DNTF. The coating effect becomes more obvious as the NC content increases. When the NC content is 5%, the friction sensitivity decreases by 72%, and a prediction formula for the exponential decay of DNTF friction sensitivity is obtained. MD calculation data show that NC can weaken the stiffness, enhance the elastic-plastic properties, increase the ductility and toughness of DNTF materials, and effectively improve the mechanical properties of DNTF. By combining experiments and simulation calculations, while considering the compatibility of new components and changes in propellant energy and other unpredictable new issues, NC can be referred to as a better coating layer for DNTF, as it has a certain feasibility for improving the friction sensitivity of DNTF.

**Keywords:** coating; friction sensitivity; desensitization; molecular dynamics



**Citation:** Yuan, J.; Qin, Y.; Liu, Y.; Sun, H.; Huang, R.; Wang, J.; Han, T.; Wu, R. Friction Sensitivity Test Experiment and Desensitization Mechanism of Nitrocellulose-Coated DNTF Explosive Crystals. *Coatings* **2023**, *13*, 1721. <https://doi.org/10.3390/coatings13101721>

Academic Editor: Michał Kulka

Received: 6 September 2023

Revised: 24 September 2023

Accepted: 27 September 2023

Published: 1 October 2023



**Copyright:** © 2023 by the authors. Licensee MDPI, Basel, Switzerland. This article is an open access article distributed under the terms and conditions of the Creative Commons Attribution (CC BY) license (<https://creativecommons.org/licenses/by/4.0/>).

## 1. Introduction

In recent years, high-energy-density materials have become a hot research topic among scholars concerning energetic materials in order to optimize the energy characteristics of propellant formulations and explosives. The new type of high-energy-density material 3,4-Bis (3-nitrofurazan-4-yl) furoxan (DNTF; Figure 1) has some comprehensive advantages, such as an excellent detonation velocity, acceptable stability, and appropriate melting point. Its comprehensive performance is superior to that of RDX and HMX and is close to that of CL-20 [1,2]. DNTF has broad application prospects in explosives, propellants, and propellants [3]. However, the high mechanical sensitivity and poor thermal stability of DNTF itself hinder its application, making it more difficult to design and produce application formulas [4].

Many scholars have conducted extensive research on reducing the mechanical sensitivity of explosives through coating. Nitrocellulose is a traditional high-energy binder with low energy and tensile strength [5,6] that is widely used in propellants [7–9]. Tappan et al. [10] introduced a method for uniformly coating CL-20 spherical nanoparticles with HDI crosslinked NC. A solid loading of up to 90% was achieved by the sol-gel synthesis frozen-gel method. Dong et al. [11] proposed a new method of coating ammonium nitrate (AN) with NC, and the results showed a decrease in impact sensitivity. Liu et al. [12] introduced a new spherical powder process method for NC-coated RDX. Shi et al. [13] prepared RDX/NC ultrafine composite energetic microspheres by spray drying with NC

as a binder. Shi et al. [14] prepared a new type of insensitive explosive by using RDX as raw material and NC as binder, using the flash evaporation method. Zhang et al. [15] successfully coated irregular HMX particles with energetic NC. In addition to using NC to modify explosives, metal powder and ignition powder are also coated and modified to obtain energetic materials with a better comprehensive performance. To protect the activity of aluminum powder in solid propellants, Liu et al. [16] used NC to coat aluminum powder and characterized its particle morphology, infrared absorption spectroscopy, laser particle size analysis, and active aluminum content. Dai et al. [17] and Jiang et al. [18], respectively, conducted NC coating modification research on ignition powder Al/Bi<sub>2</sub>O<sub>3</sub> nanothermites and zirconium powder, using NC to improve energy output and electrostatic safety. Tisdale et al. [19] prepared ultrafine pentaerythritol tetranitrate (PETN) via the spray-drying method, Xu Cong et al. [20] prepared HMX composite explosives with a 1% magnesium sulfate heptahydrate microcapsule, and Song Y et al. [21] coated CL-20 with polyquaternium-2 (M550) and graphene oxide (GO), and the friction sensitivity was significantly reduced. Zhang et al. [22] conducted a detailed analysis of various factors affecting mechanical sensitivity. Researchers at the San Diego National Laboratory [23] in the United States developed a new type of friction sensitivity tester. The new friction sensitivity tester designed by Chang et al. [24] uses 50% and 10% ignition points to characterize the friction sensitivity of various explosives.

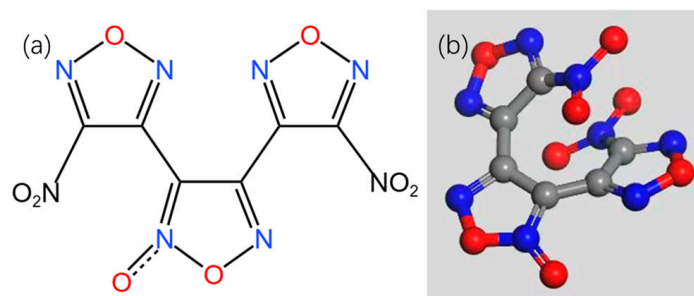


**Figure 1.** (a) The planar molecular structure of DNTF. (b) A ball–stick model of DNTF molecules.

In addition, domestic and foreign scholars have conducted some research on reducing the mechanical sensitivity and thermal sensitivity of DNTF explosives. Song et al. [25] used Am-GO as a coating to meet the mechanical sensitivity requirements of DNTF. Qin et al. [26] proposed a method of encapsulating DNTF explosive crystals with energetic binder GAP based on the water suspension method to improve their mechanical sensitivity and analyze the desensitization mechanism. In addition to coating modification with binders, DNTF and other explosives, such as DNAN, MTNP, DFTNAN, and TNBA, were optimized for mechanical sensitivity, thermal performance improvement, and energy output characteristics through the low eutectic method, respectively [27–30]. Previous research on the NC coating of other substances or explosive particles has achieved good desensitization effects, but different coating processes, experimental costs, and ease of operation have also increased many uncertainties. In this study, the coating was used between the solid propellant component binder and the oxidant explosive particles, thus avoiding the energy loss and uncertainty caused by the introduction of new coating materials. At the same time, the water suspension method for coating explosive particles is currently a traditional and widely used method, which is safe, efficient, and cost-effective, and it has strong advantages in the preparation process of molding powder.

The energetic binder NC was used as the coating material based on the water suspension method to coat DNTF explosive grains to prepare molding powder grains in this study. The morphology characteristics, thermal behavior, and friction sensitivity of the test samples coated by NC were studied. The experimental phenomenon of the ignition response in friction sensitivity testing was captured using a high-speed camera, and its changing characteristics were analyzed. The molecular dynamics simulations were ap-

plied to calculate and analyze the interface binding energy and macroscopic mechanical properties of the molecular model for NC and DNTF composite system. Combining the experimental and calculation results, the coating results of energetic polymer binder NC on DNTF explosive grains were analyzed, thus providing certain experimental and theoretical support for the optimization of the friction sensitivity of DNTF. On the basis of the friction sensitivity test results, a combination of high-speed photography results of the friction ignition response, molecular dynamics calculation results, and microscopic characterization results of the coating materials was used to analyze the friction-sensitivity reduction mechanism of NC-coated DNTF explosive grains from macro, micro, and micro perspectives.

## 2. Materials and Methods

### 2.1. Materials and Instruments

**Materials:** DNTF, purity greater than 99%, prepared by Xi'an Institute of Modernization (Xi'an, China); NC, with a nitrogen content of 13%, China North Chemical Industry Group Co., Ltd. (Beijing, China); and ethyl acetate, China National Pharmaceutical Group Chemical Reagent Co., Ltd. (Beijing, China).

**Instruments:** PTY-A electronic analytical balance, purchased from Guangzhou Shangbo Electronic Technology Co., Ltd. (Guangzhou, China); HH-S1 constant temperature water bath pot, produced by Gongyi Yuhua Instrument Co., Ltd. (Zhengzhou, China); BGX-70L electric constant temperature drying oven, produced by Suzhou Taiyoute Machinery Manufacture Co., Ltd. (Suzhou, China); SEM-30 PLUS scanning electron microscope, Beijing Tianyao Technology Co., Ltd. (Beijing, China); friction-sensitivity testing instrument MGY-I, Shanxi Institute of Applied Physics and Chemistry (Xi'an, China); and high-speed industrial camera, Shenzhen Huagu Power Technology Co., Ltd. (Shenzhen, China).

### 2.2. Preparation Experiment of NC-Coated DNTF

The coated samples were prepared with different NC contents according to the DNTF: NC mass ratios of 99:1, 98:2, 97:3, 96:4, and 95:5, respectively. DNTF was mixed with water in a ratio of 1:7 to prepare a water suspension and then stirred in a constant-temperature water bath at 60 °C for 20 min. Then, the mixture of nitrocellulose and ethyl acetate was added dropwise to the water suspension and stirred for 1 h, at a stirring rate of 300 rpm/min. After stirring, the sample was filtered through vacuum for 15 min and baked in a water-bath oven at 50 °C for 2 h to obtain the sample product. The flowchart and schematic diagram of the coating experiment are shown in Figure 2.

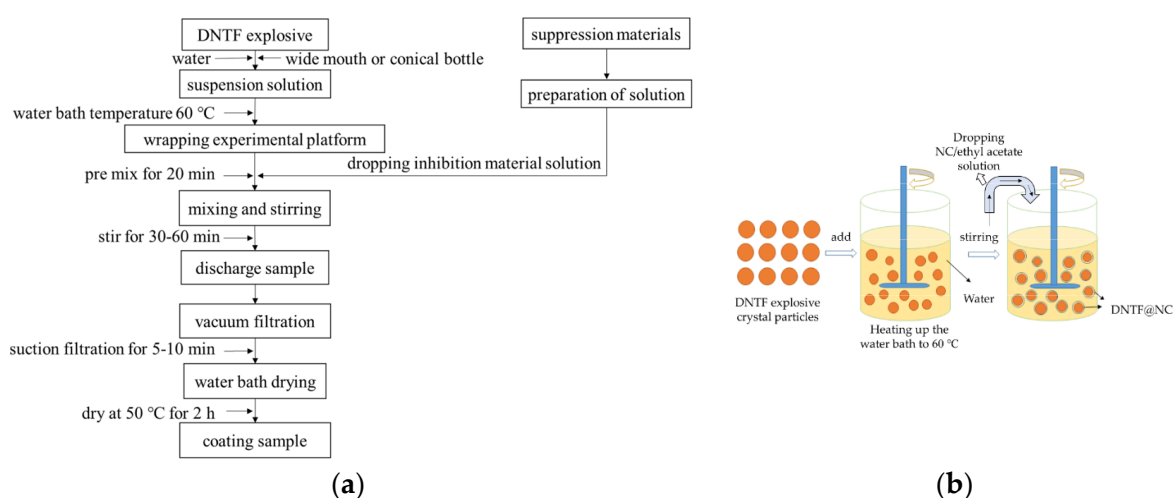


**Figure 2.** (a) The flowchart of the coating experiment. (b) The schematic diagram of the principle of the coating experiment.

### 2.3. Performance Characterization

SEM: The NC-coated grain morphology of the test sample was measured using scanning electron microscopy (SEM), and the comparative analysis was conducted on the characterization morphology of NC-coated DNTF sample and DNTF raw grains. The test samples of NC-coated DNTF explosive grains were all sprayed with gold and set to a voltage of 15 kV.

Friction sensitivity: We referred to method 602.1 of GJ772A-97 and used the MGY-I friction sensitivity instrument to test DNTF raw samples and NC-coated DNTF grains. The test gauge pressure of the friction sensitivity instrument is 2.5 MPa, the swing angle of pendulum is  $66^\circ$ , the dosage is 20 mg, and the friction sensitivity test results are expressed as the explosion rate. Parameter settings for high-speed photography industrial camera: The image resolution is  $640 \times 480$ , and the frame rate is 816 FPS. The schematic diagram of the friction sensitivity experiment principles is shown in Figure 3.

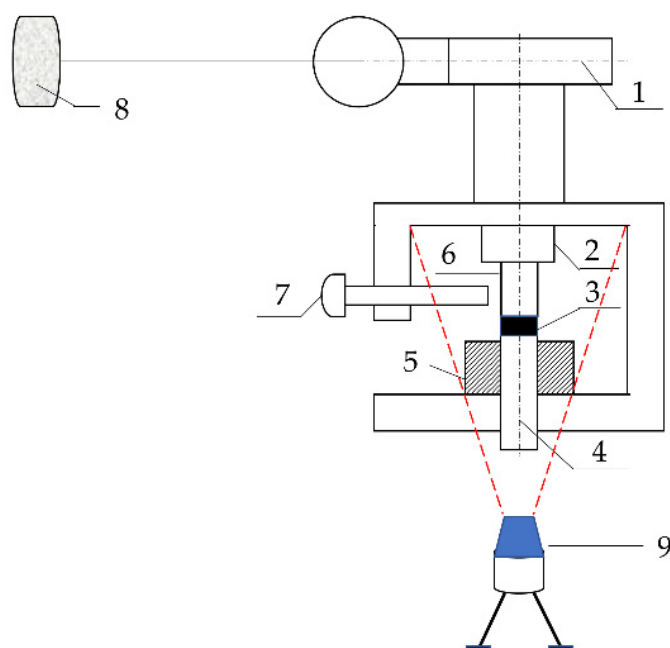


**Figure 3.** Schematic diagram of friction sensitivity experiment principle: (1) pendulum support, (2) top pillar, (3) sample, (4) punch, (5) guide sleeve, (6) upper sliding column, (7) strike rod, (8) pendulum, and (9) high-speed camera.

DSC: The thermal behavior and decomposition process of the samples were measured and analyzed using the HQC-1 differential thermal analyzer. DNTF and NC-coated DNTF samples were subjected to DSC testing and analysis at a temperature-rise rate of  $10^\circ\text{C}/\text{min}$ . Temperature test range:  $30\text{--}350^\circ\text{C}$ . Sample size:  $3 \pm 0.1$  mg. Sealed alumina crucible; empty crucible as reference material.

### 2.4. Molecular Dynamic Simulation

Referring to Reference [31], the Visualizer module in Materials Studio2019 software was used to establish DNTF  $4 \times 3 \times 3$  supercell structures that were cut along the main growth planes to construct vacuum-free crystal structures of DNTF (011), (101), and (002) crystal planes. The amorphous structure of NC was constructed based on its lattice size, and the Build Layers function was used to obtain their double-layer interface crystal model, with a vacuum layer thickness set to 30. The model was established as shown in Figure 4, where the number of AC box layers is applied to characterize the different contents of NC.

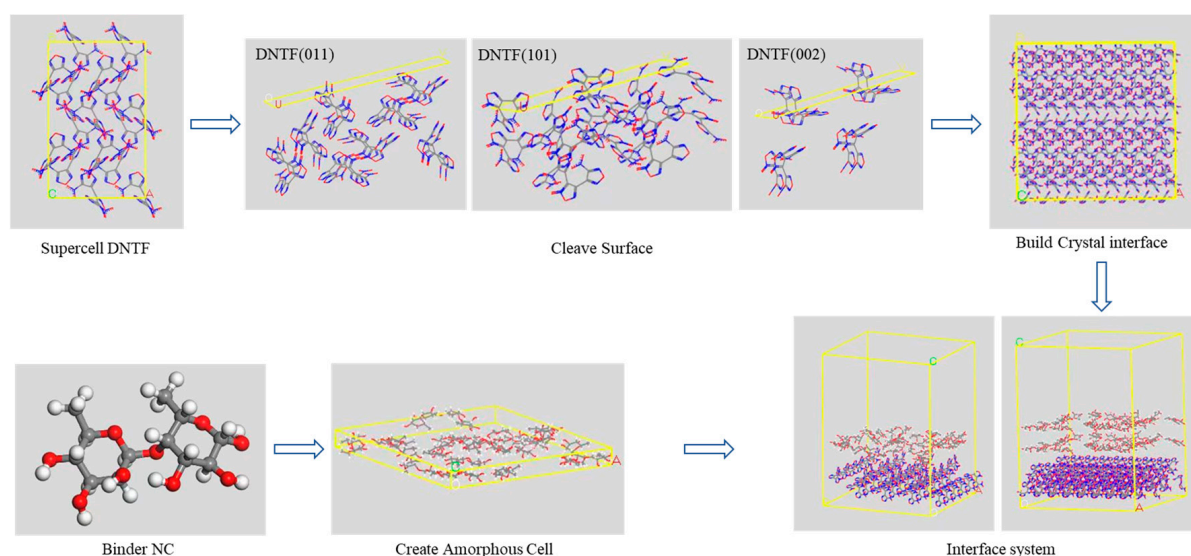


**Figure 4.** The process of establishing an interface molecular model.

The geometric structure of the established interface molecular model was optimized, and an MD simulation was performed under an isothermal isobaric ensemble (NVT) based on the optimized interface model. The simulation conditions are set as the steps below. The temperature control method is Anderson, with a time step of 1.0 fs, and a total calculated time of 200 ps. The first 100 ps time steps are employed for thermodynamic equilibrium, and the last 100 ps time steps are applied for the statistical analysis. During the molecular dynamic simulation process, the Van Der Waals force and the electrostatic interaction were calculated through Atom-based and Ewald methods, respectively. The calculated results were output once per 1000 steps, totaling 50 frames. When the fluctuation range of temperature and energy of molecular model is  $\leq 5\%$ , the system reaches dynamic equilibrium. By analyzing the molecular equilibrium structure, the binding energy and mechanical performance parameters can be obtained between the NC and DNTF composites' system.

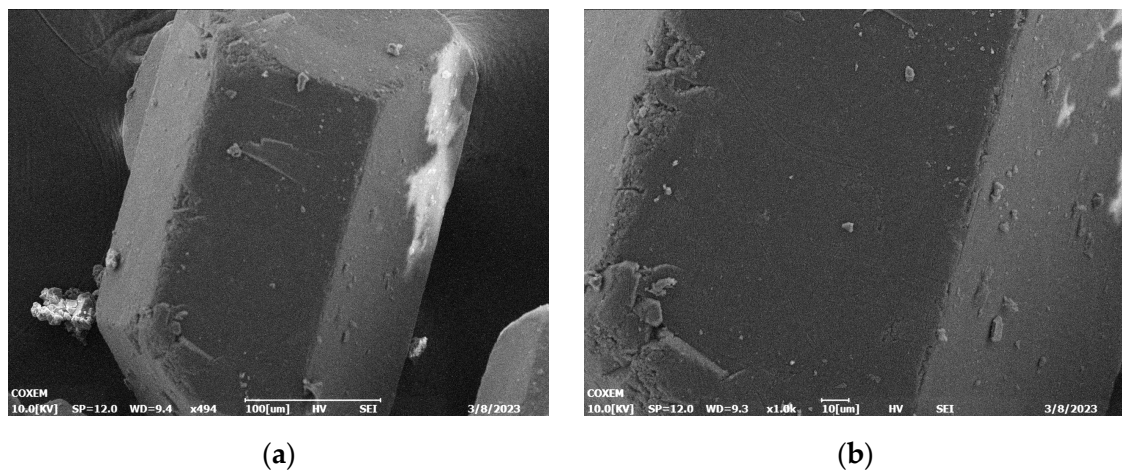
### 3. Results and Discussion

#### 3.1. Electron Microscopy Morphology Characterization

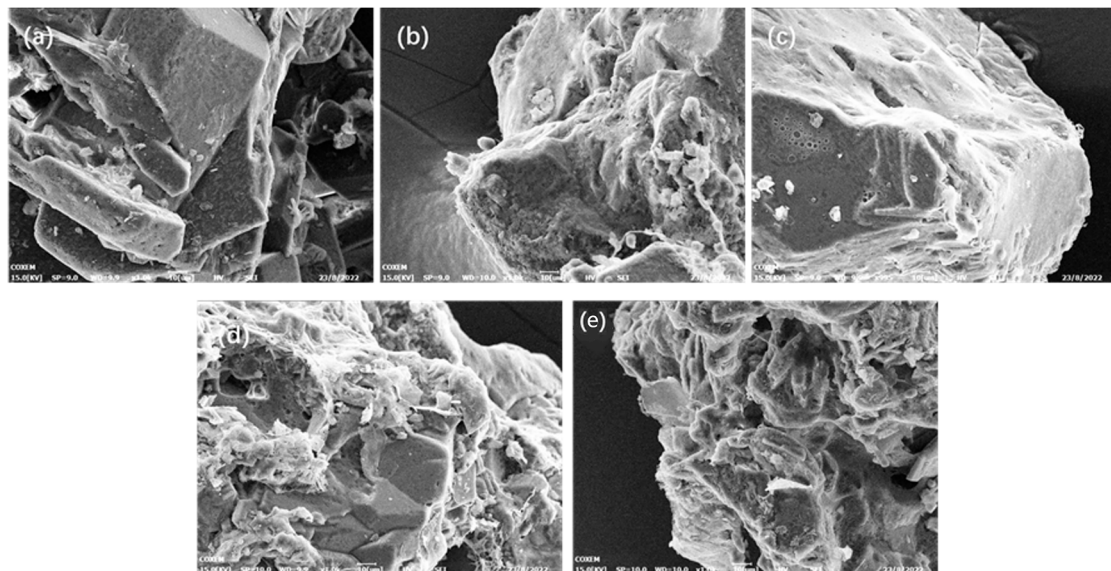
SEM was applied to characterize the microstructure of DNTF explosive grains mixed with low-melting-point explosive particles. The electron microscope photos of the morphology characteristics of DNTF grains are shown in Figure 5a,b, respectively, whose photos of DNTF grains were magnified by 500 and 1000 times. Overall, DNTF crystal particles appear in a regular polyhedral shape. The surface of DNTF grains without coating material is relatively smooth and clean, with slightly smaller grains attached to larger grain surface and no other attachments.

Figure 6 shows the electron microscopy morphology of the coating grains with a magnification of 1000 for 1% to 5% NC in subgraphs a–e.

It can be observed that, after being coated with NC, the surface roughness of DNTF increases. NC adheres smaller grains of DNTF to the surface of larger grains, and after being magnified, it can be seen that the surface of the raw DNTF grains is in an ivory adhesive condition, with a thin layer of NC evenly covering the grain surface. As the NC content increases, the ivory gel on the grain surface of the DNTF explosive becomes more obvious. The coating effect becomes more significant. The coating integrity and the thickness of the ivory gel layer on the crystal surface increase. The observed results of NC-coated DNTF grains are consistent with the increase of different crystal planes under the condition of MS vacuum, indicating that NC-coated DNTF crystals have an excellent coating effect.



**Figure 5.** The SEM morphology of DNTF raw grains: (a) 500 $\times$  and (b) 1000 $\times$ .



**Figure 6.** The morphology of coating samples (a) with 1% NC, (b) with 2% NC, (c) with 3% NC, (d) with 4% NC, and (e) with 5% NC.

### 3.2. Friction Sensitivity Test and Friction Response Analysis

The friction sensitivity test results of DNTF and NC-coated DNTF explosive samples are indicated in Table 1.

**Table 1.** Results of friction sensitivity tests.

Sample	Friction Sensitivity
DNTF	100%
$M_{\text{DNTF}}:M_{\text{NC}} = 99:1$	72%
$M_{\text{DNTF}}:M_{\text{NC}} = 99:2$	52%
$M_{\text{DNTF}}:M_{\text{NC}} = 99:3$	40%
$M_{\text{DNTF}}:M_{\text{NC}} = 99:4$	32%
$M_{\text{DNTF}}:M_{\text{NC}} = 99:5$	28%

The friction sensitivity data in Table 1 show that the friction sensitivity of DNTF explosive crystals coated with NC decreases compared to pure DNTF. When the NC content increases, the friction sensitivity of the coating system gradually decreases exponentially, as

shown in Figure 6. Based on the results of electron microscopy morphology characterization, as the NC content increases, the ivory gel on the surface of DNTF explosive grains becomes more obvious. The corresponding result is that the coating effect on DNTF crystals becomes more significant. The coating integrity and the thickness of the ivory gel layer on the crystal surface increase can reduce the heat energy generated by friction between DNTF explosive grains and the contact surface. Therefore, the explosion rate of friction ignition was decreased, and the safety performances of DNTF explosive were improved.

Based on the friction sensitivity data in Table 1, the Origin2022 software was applied to perform a scatter plot and fit the friction sensitivity prediction formula with changes in NC content, as shown below in Figure 7. The fitted exponential equation is as follows:

$$P = 97.83e^{-0.286 \cdot x}$$

where  $P$  is the probability of explosion, %; and  $x$  is the NC content and  $\leq 5$ , %.

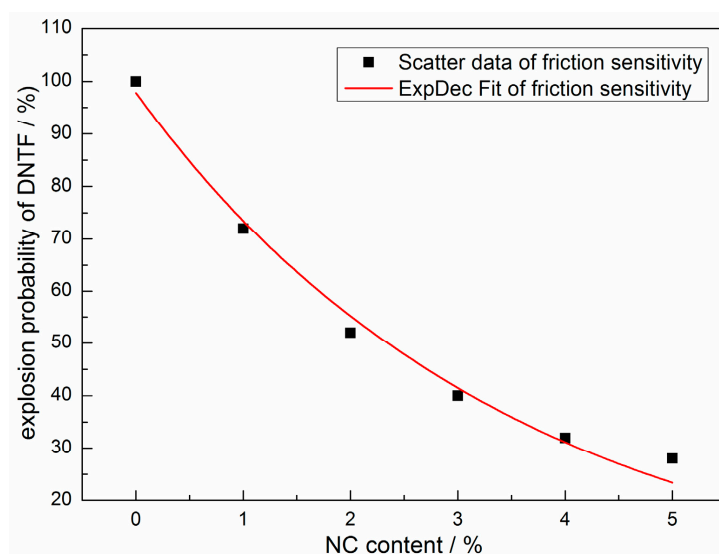


**Figure 7.** Scatter plot and fitting curve of friction sensitivity data for NC-coated DNTF.

Similar to many explosive performance studies, the explosion probability method was used to test and calculate the friction sensitivity. In addition, based on the friction sensitivity data, a prediction formula for the degree of friction sensitivity as the NC content changed was fitted, and an industrial high-speed photography camera was used to record the ignition and explosion phenomena of DNTF explosive particles and coated samples under friction to better analyze the desensitization mechanism of NC on DNTF explosive particles.

The friction sensitivity data of DNTF explosives and their coated samples were obtained through friction sensitivity testing experiments. At the same time, based on the experimental method in Figure 3, high-speed photography industrial cameras were used to capture the ignition and explosion phenomenon of the samples under friction. During the experimental testing process, the image resolution parameters of the high-speed photography industrial camera were  $648 \times 480$ , and the frame rate was 816 FPS. Therefore, the time interval between two high-speed photography images is about 1.23 ms, and the shooting time of each image can be determined by counting the image intervals. Figure 8 shows high-speed photographic images of pure DNTF grains igniting and exploding under friction experimental conditions. When  $t = 0$  ms, the hitting rod precisely contacts the upper sliding column at this moment. When  $t = 1.23$  ms, pure DNTF explosive grains have ignited and exhibit explosion luminescence phenomenon under the frictional force generated by the impact of the rod on the sliding column. When  $t = 2.46$  ms, the explosion sound and flame phenomenon disappear, and the smoke of the explosion product appears and spreads everywhere.

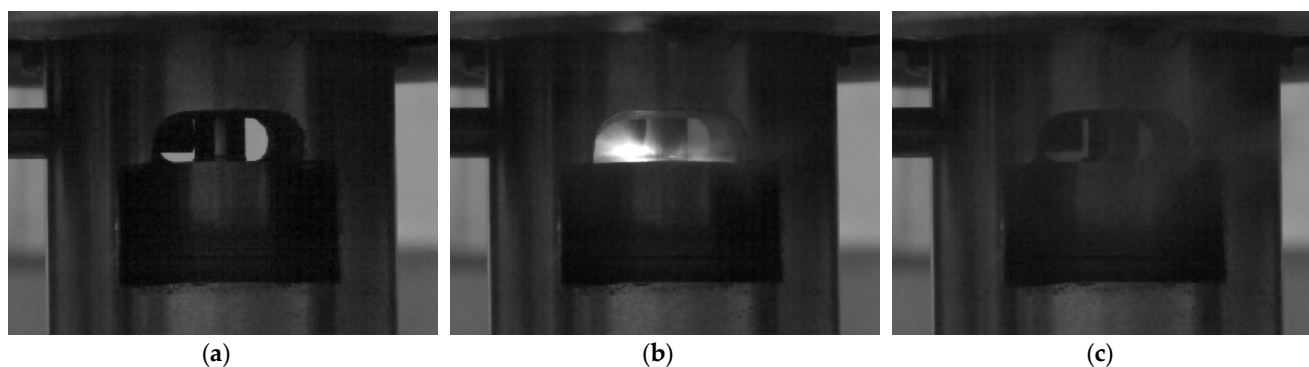


**Figure 8.** Photography of ignition and explosion of pure DNTF grains under friction: (a)  $t = 0$  ms, (b)  $t = 1.23$  ms, and (c)  $t = 2.46$  ms.

From Figure 8b, it can be seen that the pure DNTF explosive grain ignites and explodes under friction at the left end between the sliding columns. That is to say, when the sliding friction effect is just generated on the upper sliding column, the pure DNTF explosive grain immediately ignites, resulting in explosion and firelight. The phenomenon of ignition and explosion occurring at the initial stage of sliding friction indicates that pure DNTF explosive grains have high friction sensitivity, high energy release efficiency, and high danger. At the experimental site, it was found that the sample had a loud explosion sound under the action of friction, and there was a visible flame phenomenon in the explosion chamber, which is basically consistent with the analysis of the experimental phenomenon taken by high-speed photography in Figure 6. This indicates that the phenomenon of high-speed photography is in good agreement with the phenomenon that occurs after friction ignition of the experimental site sample, and the analysis conclusion is also scientifically reliable.

Figure 9 shows a series of high-speed captured images of pure DNTF explosive grains ignited and weakly exploded under friction. Figure 9a–c are three consecutive images taken during the initial ignition of DNTF grains. There is obvious smoke in the photos, indicating that the primary ignition of explosive grains occurred and that they began to decompose. Figure 9d–f show the product and residual sample flying in a relatively enclosed space after the hitting rod rebounds and leaves the upper sliding column, accompanied by smoke. After conducting the analysis, we noted that the phenomenon of the weak explosion of pure DNTF explosive grains in Figure 9 is consistent with the fact that the explosive sample in the experimental site produced a crisp explosion sound. These explanations are reasonable for the analysis process and results of ignition, decomposition, and weak explosion of the sample in Figure 9.

Based on the water suspension method, a feasibility study was conducted on the desensitization of DNTF explosive grains coated with energetic binder NC. The friction sensitivity experimental data in Table 1 show that this desensitization method is feasible. NC is an energetic polymer material that can also reduce the energy loss of the explosive composite system caused by the increase of the coating material. Meanwhile, although the friction sensitivity test results of the samples coated with DNTF in NC in Table 1 gradually decrease with the increase of NC content, there is still a certain probability of explosion. Therefore, the sample coated with DNTF by NC will also undergo ignition, decomposition, and explosion under the action of friction, only reducing the probability of explosion in a statistical sense. Thus, Figure 10 shows high-speed photography images of the ignition and explosion of the coating material sample with a content of 3% NC under friction. From Figure 10b, it can be seen that the flame phenomenon occurs at the right end between the sliding columns during the ignition explosion of the 3% NC coating material sample. This indicates that the ignition and explosion phenomena of the sample after friction are somewhat delayed. This ignition phenomenon is exactly opposite to the ignition explosion of the pure DNTF grain sample in Figure 8b at the left end between the sliding columns. The subtle difference in ignition and explosion time indicates that the ignition response

time of DNTF explosive grains coated with NC is delayed under the action of friction. This indirectly confirms that NC, as a coating desensitizing material, plays a role in delaying or reducing the friction sensitivity of DNTF explosives.

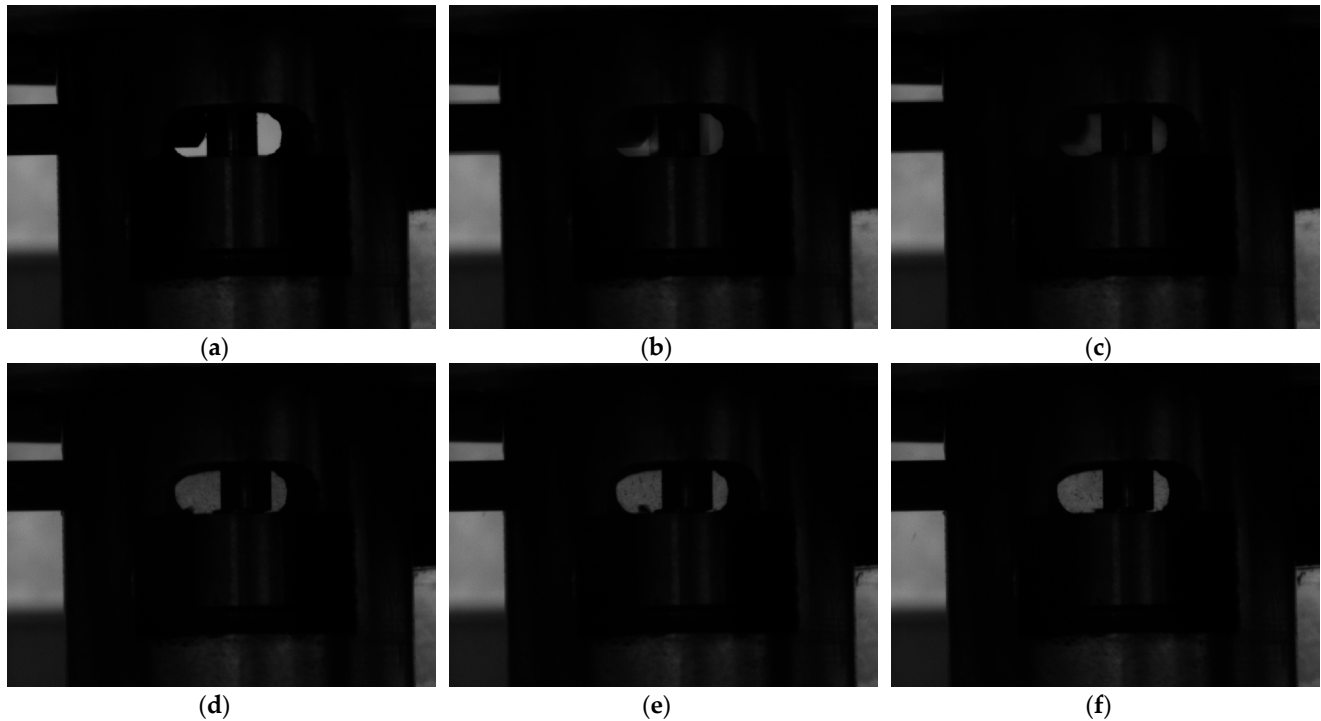


**Figure 9.** Photography of ignition and smoke emission of pure DNTF grains under friction: (a)  $t = 0$  ms, (b)  $t = 1.23$  ms, (c)  $t = 2.46$  ms, (d)  $t = 9.84$  ms, (e)  $t = 13.53$  ms, and (f)  $t = 17.22$  ms.

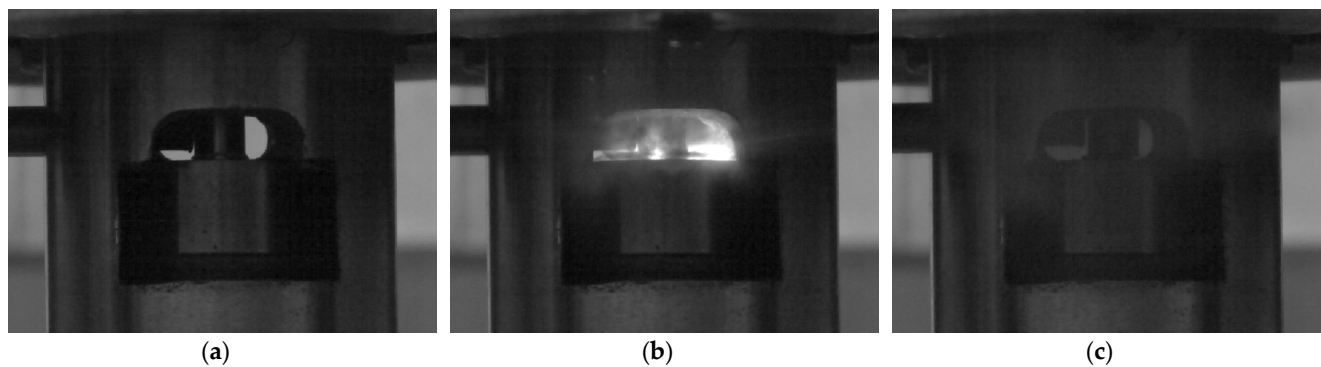


**Figure 10.** Photography of ignition and explosion of NC-coated DNTF grains with 3% NC content under friction: (a)  $t = 0$  ms, (b)  $t = 1.23$  ms, and (c)  $t = 2.46$  ms.

The aforementioned experimental data indicated that the explosion rate of the DNTF explosive samples coated with NC decreases with the increase of NC content under the action of friction. At the same time, even if it was judged that the explosive sample coated with NC is explosion, the experimental phenomenon was mainly caused by the ignition decomposition of the sample, as shown in Figure 11, and accompanied by smoke, while the ignition explosion phenomenon shown in Figure 10b was relatively rare.

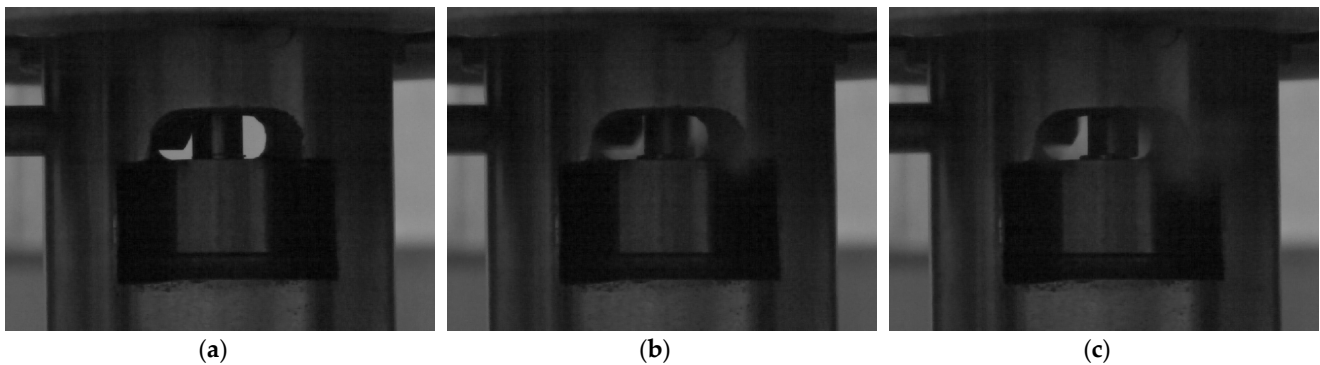


**Figure 11.** Photography of ignition and smoke emission of NC-coated DNTF grains with 3% NC content under friction: (a)  $t = 0$  ms, (b)  $t = 1.23$  ms, and (c)  $t = 2.46$  ms.

Figure 11 shows that the coated DNTF explosive sample with a 3% NC content underwent ignition and decomposition reactions under the experimental conditions in this study, resulting in a significant amount of smoke and the effect of flying out of the explosion chamber. This is the same as the smoke phenomenon observed during the friction sensitivity testing experiment, but different from the weak explosion phenomenon in the pure DNTF explosive sample in Figure 9, which leads to the scattering of products and sample residues. This also indicates that NC as a coating material can weaken the intensity of ignition response of DNTF explosives under the same friction sensitivity experimental conditions.

### 3.3. DSC Analysis

The DSC curves of pure DNTF explosives and coated samples are shown in Figure 12. According to the DSC curve, the thermal decomposition process of pure DNTF is mainly divided into two stages, including an endothermic melting stage and an exothermic decomposition stage. The endothermic peak is  $113.7$  °C, and the exothermic peak is  $279.9$  °C.

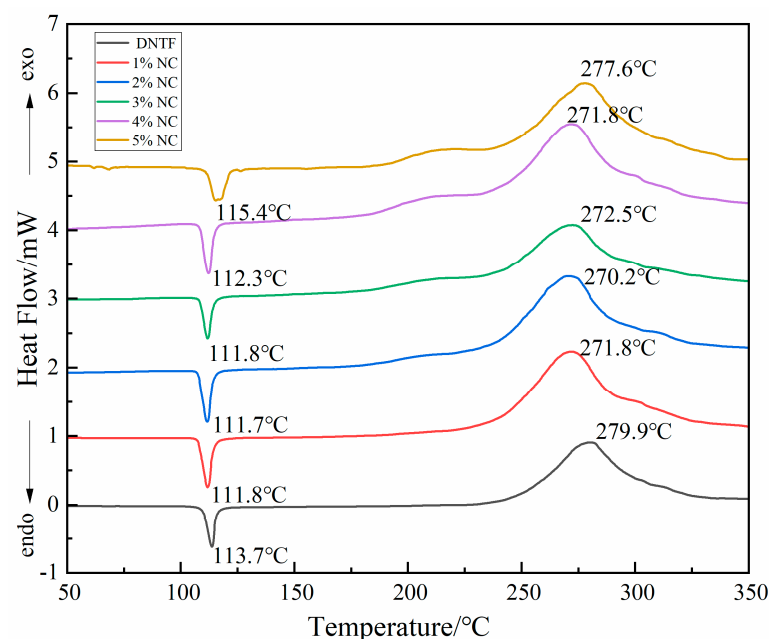


**Figure 12.** DSC curves of DNTF and coated samples.

When the NC content is between 1% and 4%, the endothermic peak corresponding to the melting process of DNTF decreases slightly. The melting process of DNTF in the

NC-coated sample is reduced, the exothermic decomposition is promoted, and the peak decomposition temperature is lower than that of pure DNTF explosives. The DSC curve shows that the NC/DNTF sample begins to undergo exothermic decomposition at about 200 °C. As the NC content increases, the temperature required for exothermic decomposition to occur decreases. When the NC content is 4% and 5%, there are two obvious heating cycles and two exothermic peaks. The 5% NC content makes the endothermic peak temperature of the coated sample higher than that of pure DNTF, and the decomposition peak temperature of the 5% NC/DNTF sample is higher than that of the other four contents. It is speculated that this may be influenced by the NC content.

### 3.4. Theoretical Calculation of Binding Energy

The last equilibrium structure calculation based on the NVT ensemble MD simulation can obtain the binding energy ( $E_{\text{bind}}$ ) of different crystal planes between the binder NC and DNTF; this calculation is commonly applied to measure the strength of the interaction forces between different components in the composite material system. The larger the value of binding energy, the more precise the binding between each component in the composite system. The stronger the interaction force, the higher the thermodynamic stability of the composite explosive system, and the more stable the formed coating structure. The calculation formula is as shown in Equation (1) [32]:

$$E_{\text{binding}} = -E_{\text{inter}} = -(E_{\text{total}} - E_{\text{DNTF}} - E_{\text{NC}}) \quad (1)$$

In the equation,  $E_{\text{inter}}$  is the interaction energy between two components;  $E_{\text{total}}$  is the total energy of the composite explosive system in equilibrium;  $E_{\text{DNTF}}$  is the single point energy of the crystal surface of DNTF explosive after the adhesive was removed; and  $E_{\text{NC}}$  is the single point energy of the adhesive after excluding the DNTF crystal surface, all in Kcal/mol. The binding energies of different crystal planes of NC and DNTF were calculated on the basis of Equation (1), and the results are all listed in Table 2.

**Table 2.** Calculation results of the interface model binding energy.

Compound System		$E_{\text{total}}/(\text{kcal}\cdot\text{mol}^{-1})$	$E_{\text{explosive}}/(\text{kcal}\cdot\text{mol}^{-1})$	$E_{\text{binder}}/(\text{kcal}\cdot\text{mol}^{-1})$	$E_{\text{binding}}/(\text{kcal}\cdot\text{mol}^{-1})$
NC/DNTF (011)	E	−6011.8	−13,019.3	908.4	−6099.1
	vdw	−1608.1	−1880.9	118.3	−391.1
	Electrostatic	−4418.9	−5739.4	1276.6	−2597.1
	E	−3989.7	−13,019.3	1780.6	−7249
	vdw	−1533.5	−1880.9	220.4	−567.8
	Electrostatic	−3271.6	−5739.4	2559.9	−5027.7
NC/DNTF (101)	E	−1971.8	−6318.6	690.0	−3656.8
	vdw	−683.2	−800.9	98.6	−216.3
	Electrostatic	−1700.9	−2822.3	1108.3	−2229.7
	E	225.2	−6318.6	1355.8	−5188
	vdw	−537.3	−800.9	172.5	−436.1
	Electrostatic	−481.4	−2822.3	2225.1	−4566
NC/DNTF (002)	E	−593.3	−4113.6	774.6	−2745.7
	vdw	−419.6	−337.8	89.6	−7.8
	Electrostatic	−782.9	−1723.0	1165.9	−2106
	E	1523.3	−4113.6	1489.2	−4147.7
	vdw	−384.4	−337.8	133.4	−86.8
	Electrostatic	351.0	−1723.0	2342.2	−4416.2

Table 2 shows the binding energy calculations for three interface systems with different binder contents. It can be seen that the nonbonding energy in the binding energy includes two parts of the forces: vdw (van der Waals force) and electrostatic (electrostatic interaction). The contribution of electrostatic interaction energy to binding energy in the interface systems of NC/DNTF (011), NC/DNTF (101), and NC/DNTF (002) is 42.3%, 60.9%, and 76.7%, respectively. With the increase in the binder content, the contribution of electrostatic

interaction energy to binding energy becomes more obvious, illustrating that the interaction between the NC molecular structure and DNTF crystal plane is mainly the adsorption effect of electrostatic force. The binding energy values of the NC/DNTF interface system are in the order of (011) > (101) > (002). As the binder content increases, the binding energy values increase, and the binding energy values of the three NC/DNTF interface systems are greater than those of the DNTF system by 1452.3 kcal mol<sup>-1</sup>, indicating that the interface between the binder and the explosive can exist steadily. The binding energy between NC/DNTF (011) interface is the highest, displaying that the interaction strength of NC/DNTF (011) is significantly higher than that between NC/DNTF (101) and NC/DNTF (002), indicating better compatibility and stronger binding between NC and DNTF (011). The calculation results of NC/DNTF binding energy indicate that the larger the binding energy value between the DNTF crystal interface and the adhesive NC, the stronger their bonding, and the smaller the interfacial slip, which can reduce the heat energy generated by friction between the DNTF crystal and the contact area of sliding column. Therefore, the explosion rate of friction ignition response will be significantly reduced. The calculated values of the binding energy of NC/DNTF composite system match the test results well. Therefore, the friction sensitivity values of the NC/DNTF coating gradually decrease with the increase of NC content, which better reflects the internal factors that affect the friction sensitivity of DNTF as a coating layer. In addition, as mentioned in Reference [33], the numerical value of Gibbs free energy can characterize the thermal stability and toughness of the composite system. The smaller the value of Gibbs free energy, the smaller the influence of temperature on the composite system and, thus, the less likely it is to form hot spots, making it beneficial for reducing the sensitivity of NC and DNTF systems.

### 3.5. Mechanical Performance Calculation

According to Hooke's law and the stiffness matrix of the composite materials, the mechanical properties can be obtained through theoretical calculations, e.g., the stress-strain of the system ( $\sigma$ - $\epsilon$ ). The relationship satisfies the generalized Hooke's law [34,35]:

$$\sigma_i = C_{ij}\epsilon_j \quad (2)$$

Among them,  $\sigma_i$  is the stress tensor, GPa;  $\epsilon_j$  is the strain tensor, %;  $C_{ij}$  ( $i, j = 1-6$ ) is a stiffness matrix of elastic constants, representing the stress-strain relationship. The larger value of  $C_{ij}$ , the greater the stress that needs to be borne when producing the same strain. When the material is taken for an isotropic material, the stiffness matrix of the stress-strain performance can be expressed by the Lamé coefficients  $\lambda$  and  $\mu$ , as shown in Equation (3) [36,37]:

$$[C_{ij}] = \begin{bmatrix} \lambda + 2\mu & \lambda & \lambda & 0 & 0 & 0 \\ \lambda & \lambda + 2\mu & \lambda & 0 & 0 & 0 \\ \lambda & \lambda & \lambda + 2\mu & 0 & 0 & 0 \\ 0 & 0 & 0 & \mu & 0 & 0 \\ 0 & 0 & 0 & 0 & \mu & 0 \\ 0 & 0 & 0 & 0 & 0 & \mu \end{bmatrix} \quad (3)$$

The static mechanical performance analysis on the NVT ensemble under equilibrium state was performed, and the elastic coefficients ( $C_{ij}$ ) and effective isotropic moduli of different crystal interface models were obtained for NC and DNTF, including the Young's modulus (E), shear modulus (G), bulk modulus (K), K/G value, and Cauchy pressure ( $C_{12} - C_{44}$ ). According to the correlation system between the moduli of isotropic materials, the Latin American coefficient is used,  $\lambda$  and  $\mu$ , represented as follows [38,39]:

$$E = \frac{\mu(3\lambda + 2\mu)}{\lambda + \mu} \quad (4)$$

$$K = \lambda + \frac{2}{3}\mu \quad (5)$$

$$G = \mu \quad (6)$$

$$\gamma = \frac{\lambda}{2(\lambda + \mu)} \quad (7)$$

According to Equation (8), the Poisson's ratio of the NC/DNTF composite system can be calculated ( $\nu$ ). The calculation results of various moduli are illustrated in Table 3.

$$E = 2G(1 + \nu) = 3K(1 - 2\nu) \quad (8)$$

**Table 3.** Mechanical performance parameters of interface system.

Modules/GPa	NC/DNTF (011)	NC/DNTF (101)	NC/DNTF (002)	DNTF
C <sub>11</sub>	0.5030	0.7275	0.3631	12.8557
C <sub>22</sub>	1.8968	1.0453	1.8536	10.6884
C <sub>33</sub>	−0.4392	0.7669	0.5203	9.1765
C <sub>44</sub>	−0.3052	0.5386	0.2328	2.1781
C <sub>55</sub>	−0.0539	0.7014	0.3603	2.0604
C <sub>66</sub>	−0.3401	0.5203	−0.2340	8.0035
C <sub>12</sub>	0.6586	0.8909	0.5465	3.2970
C <sub>13</sub>	−0.1685	0.2640	−0.2296	1.1050
C <sub>23</sub>	0.9194	0.1659	1.3602	3.2776
E	0.8917	1.3836	0.3410	10.4586
Γ	0.4138	0.1789	0.4245	0.1531
K	1.2751	0.7182	0.7526	5.0247
G	0.2331	0.5868	0.1197	4.5350
K/G	5.4702	1.2239	6.2874	1.1080
N	0.3834	0.1789	0.4244	0.1531
C <sub>12</sub> –C <sub>44</sub>	0.9638	0.3523	0.3137	1.1189

The plasticity and fracture properties of composite materials are closely connected to modulus. The modulus parameter of mechanical properties is an indicator for evaluating the rigidity of materials and a measure of the degree of resistance to elastic deformation. The Young's modulus (E), bulk modulus (K), and shear modulus (G) can all be applied to measure the rigidity of a composite material. The Young's modulus is a sign of material rigidity, and the higher its value, the less likely it is to undergo deformation. The bulk modulus can also be applied to represent the fracture strength of materials. The larger the value of bulk modulus, the greater the energy required for material fracture; that is to say, the fracture force of the material will correspondingly increase. The shear modulus is related to the hardness, representing the ability to prevent plastic deformation of materials. The higher the value of the shear modulus, the higher the hardness and yield strength of the composite material.

The ratio of the bulk modulus to shear modulus (K/G) is employed to measure the composite system's toughness, which is the property of the material absorbing energy because of plastic deformation. The higher the value of the bulk modulus to shear modulus (K/G), the better the toughness of the composite system. The K/G value can also be applied to evaluate the ductility of materials. The higher the value of the K/G, the better the ductility of the composite material. The Cauchy pressure (C<sub>12</sub> – C<sub>44</sub>) can also be used to assess the ductility of the composite system and reflect the degree of brittleness of the composite material. The Cauchy pressure is negative, and the composite material represents brittleness. The smaller the negative value of the Cauchy pressure, the stronger the brittleness of the composite material. On the contrary, when the Cauchy pressure becomes positive, it means that the material has good ductility and exhibits excellent toughness. Poisson's ratio ( $\nu$ ) denotes the ratio of transverse and longitudinal strains as a result of load. The parameters of mechanical performance for the different crystal interface systems of adhesive NC/DNTF and pure DNTF are illustrated in Table 3.

Referring to the various parameters of the DNTF crystal, it can be found that the energetic binder NC effectively improves the modulus of isotropic material of DNTF crystal. Compared to the modulus of pure DNTF crystals, the tensile modulus (E), bulk modulus (K), and shear modulus (G) of NC/DNTF (011), NC/DNTF (101), and NC/DNTF (002) composite systems decrease, indicating a decrease in the hardness, yield strength, and fracture strength of NC/DNTF composite material; a decrease in the rigidity; an increase in the elastoplasticity; and an increase in the Poisson's ratio [37]. The  $K/G$ ,  $\gamma$ , and  $\nu$  values of NC/DNTF (011) surface system, NC/DNTF (101) surface system, and NC/DNTF (002) surface system are all higher than those of pure DNTF crystals, and the  $C_{12} - C_{44}$  values of the three composite systems are all positive. Therefore, it can be inferred that the binder NC can optimize the ductility of DNTF and make DNTF have good toughness. Based on the above analysis, it can be concluded that NC as the coating material of DNTF can obviously optimize the mechanical properties of DNTF, especially the increase of elastoplastic performance of the material system, which can effectively reduce the friction ignition caused by interface friction of DNTF. This indicates that the friction sensitivity of NC/DNTF coating gradually decreases with the increase in NC content, mainly because NC as the coating layer significantly raises the elastoplastic mechanical properties of DNTF. Therefore, the calculation results of molecular dynamics for assessing the mechanical properties of the NC/DNTF composite material well reflect the essential reason for the significant decrease in the friction sensitivity of the NC/DNTF coating at the macro level. The modulus parameters of the NC/DNTF composite system contained with a double-layer adhesive are illustrated in Table 4.

**Table 4.** Parameters of mechanical property between NC/DNTF interfaces.

Modules/GPa	NC/DNT (011)	NC/DNT (101)	NC/DNT (002)	DNTF
E	0.5641	0.9435	0.6997	10.4586
$\Gamma$	0.1972	0.3353	0.3158	0.1531
K	0.3105	0.9548	0.6330	5.0247
G	0.2356	0.3533	0.2659	4.5350
K/G	1.3179	2.7025	2.3806	1.1080
N	0.1972	0.3353	0.3157	0.1531
$C_{12}-C_{44}$	0.2964	0.3090	0.3534	1.1189

When the adhesive is set to two layers, the E, K, G, and  $C_{12} - C_{44}$  values of the interface crystals of NC/DNTF (101) and NC/DNTF (002) are larger than those of the NC/DNTF (011) composite material. As the content of the binder NC increases, the mechanical properties of the composite material tend to stabilize. As the first long surface of the crystal, the mechanical modulus of the corresponding interface system on the DNTF (011) surface is smaller than that on the corresponding interface systems on the DNTF (101) and NC/DNTF (002) surfaces, thus proving to be a good way of increasing the mechanical properties of DNTF [37].

### 3.6. Analysis on Desensitization Mechanism of Friction Sensitivity of NC-coated DNTF

NC itself is one of the important energetic binders in the formulation design of explosives, and there is no need to choose new materials as the coating of DNTF crystals to avoid other new problems involving things such as compatibility, energy reduction, and unpredictability. The practical preparation process also shows that the molding powder granules prepared by DNTF explosive and NC through the water suspension method have a solid and high-density layer with similar spherical characteristics. The practical photos of pure DNTF explosive and NC-coated DNTF explosive materials are shown in Figure 13. Among them, the particle size range of pure DNTF explosives in Figure 13a is mainly between 100 and 300  $\mu\text{m}$ , and the color is light yellow. The particle size of the NC-coated DNTF material sample in Figure 13b is mainly around 1 mm. Figure 14 shows photos of two typical coated particles under a microscope.

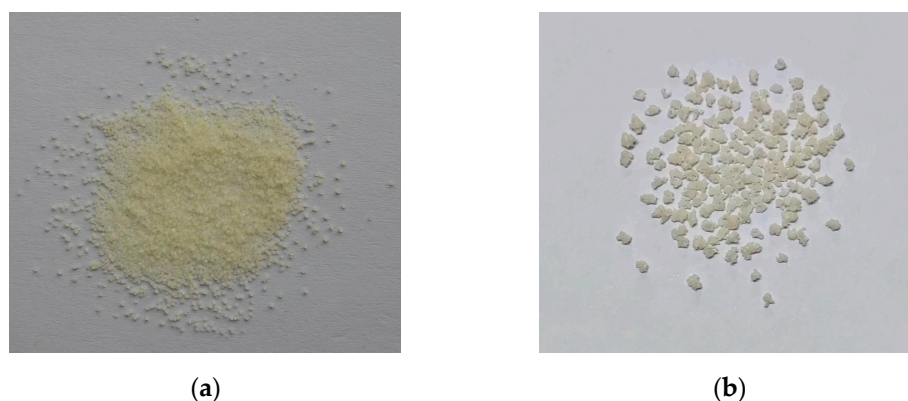


**Figure 13.** The practical photos of pure DNTF and NC-coated samples. (a) DNTF raw material and (b) NC-coated DNTF sample.

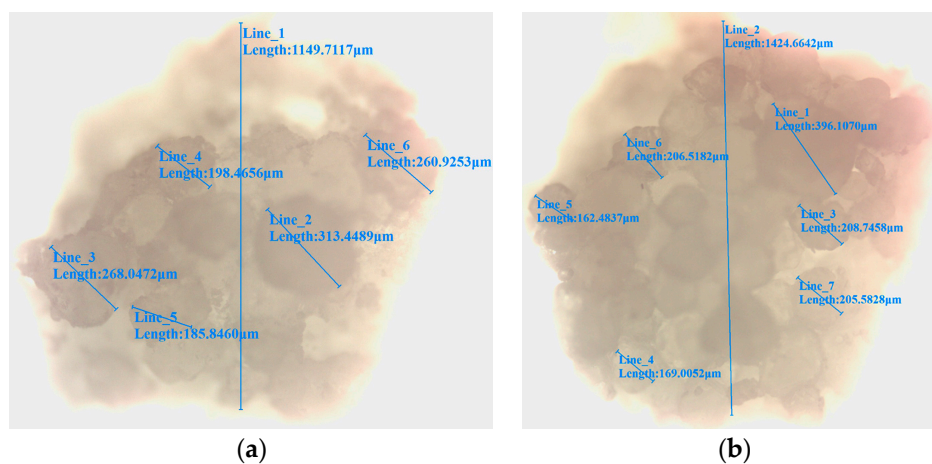


**Figure 14.** Microscopic photos of NC-coated DNTF samples. (a) NC-coated DNTF particle sample 1. (b) NC-coated DNTF particle sample 2.

It can be seen from Figure 14 that the particle size of the coated sample in Figure 14a is about 1.147 mm, while in Figure 14b, the particle size of the coated sample is about 1.45 mm, and each coated sample contains multiple DNTF explosive grains. The electron microscope scanning photos in Figure 6 indicate that a single grain surface of DNTF is coated with an NC layer of milky-white coating material. However, it can also be seen from Figure 14 that the finished product of the NC-coated DNTF material sample prepared in the laboratory is actually composed of multiple DNTF explosive grains containing NC-coating layers. The coated sample is wrapped and adhered together in a water-suspended turbulent liquid through an NC binder. This wrapping effect can enhance the sense-reducing effect of DNTF.

The quasi-static normal compression process of molding powder granules exhibits three stages: elastic deformation, elastoplastic deformation, and failure collapse [40]. When subjected to frictional force, the molding powder granules formed by the energetic coating NC with elastic characteristics and DNTF explosive crystals first absorb most of the external stimulation energy, prolonging the elastic deformation process of DNTF explosive crystals. Secondly, the good bonding performance of the interface between NC and DNTF crystals will effectively prevent the interface slip between NC and DNTF crystals, making the molding powder granules less prone to cracking and energy dissipation during the elastoplastic deformation process, effectively suppressing the generation of hot spots, and reducing the probability of ignition and explosion. Finally, the approximately spherical NC-coated DNTF explosive molding powder granules have no edges and a large specific surface area, which dissipates heat quickly when friction with a rigid interface makes it harder to generate local high temperatures to form hot spots. Therefore, the energetic

binder NC-coated DNTF explosive crystal, which is widely used in the field of explosives, is an optimal method for reducing sensitivity. There are certain limitations in the actual coating preparation. The particle size of DNTF crystals is small, and due to the good adsorption of the energetic binder NC, the samples prepared in the laboratory are actually composed of many smaller DNTF grains coated with NC which are difficult to form into spherical powders.

#### 4. Conclusions

- (1) The surface of pure DNTF is relatively smooth and flat, and the surface of DNTF coated with NC has a layer of white gel. With the increase in NC content, the white gel becomes more obvious, and the coverage and thickness of the coating increase, indicating that NC has a good coating effect on DNTF crystals.
- (2) NC can significantly reduce the sensitivity of DNTF, and with the growth of the NC content, the friction sensitivity of the NC/DNTF explosive material exponentially decreases. This desensitization mechanism is that, as the NC content of the coating layer increases, NC-coated DNTF grains can effectively absorb energy, reduce frictional tearing between interfaces, and play a buffering role when subjected to external mechanical stimulus for optimizing the safety performance of DNTF explosives.
- (3) The binding energy of the NC/DNTF (011) system is higher than that of the NC/DNTF (101) and NC/DNTF (002) systems, revealing that NC has better compatibility with DNTF (011) and binds more firmly and stably. With the rise in NC content, the binding energy value of the composite material increases, and this is consistent with the numerical value of single-layer NC binding energy. The large binding energy of the NC/DNTF interface is one of the primary internal reasons for the significant decrease in its explosion rate of friction sensitivity.
- (4) The molecular dynamics calculation results indicate that the binder NC apparently updates the isotropic material modulus of DNTF explosive materials, reducing their rigidity and enhancing their flexibility. DNTF has good ductility and toughness, making it beneficial for reducing the sliding friction heat generated between DNTF and the contact interface. Therefore, the explosion rate of the friction sensitivity test will be significantly lower.

In summary, NC can serve as a good energetic coating layer for DNTF to prepare molding powder granules. The experimental results and theoretical simulation calculations also indicate that NC has a significant and feasible reduction effect on the friction sensitivity of DNTF.

**Author Contributions:** Conceptualization, J.Y.; methodology, J.Y.; validation, Y.Q., H.S. and Y.L.; formal analysis, H.S., Y.L. and R.H.; data curation, J.W. and T.H.; writing—original draft preparation, Y.Q. and J.Y.; writing—review and editing, J.Y. and Y.Q.; visualization, R.H., J.W., T.H. and R.W. All authors have read and agreed to the published version of the manuscript.

**Funding:** This research was funded by Robust Munitions Center, CAEP (No. RMC2014B03), and the Bottleneck Technology foundation (No. 20210579).

**Institutional Review Board Statement:** Not applicable.

**Informed Consent Statement:** Informed consent was obtained from all subjects involved in the study.

**Data Availability Statement:** The data presented in this study are openly available.

**Conflicts of Interest:** The authors declare no conflict of interest.

#### References

1. Hu, H.X.; Zhang, Z.Z.; Zhao, F.Q.; Xiao, C.; Wang, Q.H.; Yuan, B.H. A Study on the Properties and Application of High Energy Density Material DNTF. *Acta Armamentarii* **2004**, *25*, 155.
2. Zheng, W.; Wang, J.N.; Ren, X.N.; Zhang, L.Y.; Zhou, Y.S. An Investigation on Thermal Decomposition of DNTF-CMDB Propellants. *Propellants Explos. Pyrotech.* **2010**, *32*, 520–524. [[CrossRef](#)]

3. Zou, Z.; Zhao, F.; Zhang, M.; Tian, J.; Wang, X. Research Progress of 3,4-Dinitrofurazanfuroxan Performances and Its Applications. *Explos. Mater.* **2019**, *48*, 11–16.
4. Li, Y.; Yuan, J.M.; Zhao, W.; Qu, Y.; Xing, X.W.; Meng, J.W.; Liu, Y.C. Application and Development of 3, 4-Bis (3-nitrofurazan-4-yl) furoxan (DNTF). *Russ. J. Gen. Chem.* **2021**, *91*, 445–455. [[CrossRef](#)]
5. Chen, P.; Ding, Y. Mechanical behaviour and deformation and failure mechanisms of polymer bonded explosives. *Energy Mater.* **2000**, *8*, 161–164.
6. Liu, C.; Zhang, L.H.; Yang, P.H. Effect of macromolecule toughening agent on the anti-impact properties of nitramine gun propellant. *Chin. J. Explos. Propellants* **2015**, *38*, 82–86.
7. Zhang, W.; Fan, X.Z.; Wei, H.J.; Li, J.Z. Application of Nitramines Coated with Nitrocellulose in Minimum Signature Isocyanate-Cured Propellants. *Propellants Explos. Pyrotech.* **2008**, *33*, 279–285. [[CrossRef](#)]
8. Chelouche, S.; Trache, D.; Tarchoun, A.F.; Abdelaziz, A.; Khimeche, K. Compatibility assessment and decomposition kinetics of nitrocellulose with eutectic mixture of organic stabilizers. *J. Energetic Mater.* **2020**, *38*, 48–67. [[CrossRef](#)]
9. Liang, T.; Zhang, Y.; Ma, Z.; Guo, M.; Liu, C. Energy characteristics and mechanical properties of cyclotrimethylenetrinitramine (RDX)-based insensitive high-energy propellant. *J. Mater. Res. Technol.* **2020**, *9*, 15313–15323. [[CrossRef](#)]
10. Tappan, B.C.; Brill, T.B. Thermal Decomposition of Energetic Materials 86. Cryogel Synthesis of Nanocrystalline CL-20 Coated with Cured Nitrocellulose. *Propellants Explos. Pyrotech.* **2003**, *28*, 223–230. [[CrossRef](#)]
11. Dong, Q.; Jiang, R.Z.; Cui, S.M.; Dong, G. A study on coating technology of ammonium nitrate with nitrocellulose. *Chin. J. Energetic Mater.* **2011**, *5*, 114–120.
12. Liu, X.G.; Wang, K.Q.; Shao, C.B.; Yu, H.J.; Fan, X.Z. A New Method of RDX coated with Nitrocellulose. *Chin. J. Energetic Mater.* **2011**, *11*, 153–154.
13. Shi, X.F.; Wang, J.Y.; Li, X.D.; Wang, J. Preparation and properties of RDX-based composite energetic microspheres. *Chin. J. Energetic Mater.* **2015**, *23*, 428–432.
14. Shi, X.; Wang, J.; Li, X. Preparation and properties of RDX-nitrocellulose microspheres. *Cent. Eur. J. Energetic Mater.* **2016**, *13*, 871–881.
15. Zhang, Y.J.; Bai, Y.; Li, J.Z.; Fu, X.L.; Yang, Y.J.; Tang, Q.F. Energetic nitrocellulose coating: Effective way to decrease sensitivity and modify surface property of HMX particles. *J. Energetic Mater.* **2019**, *37*, 212–221. [[CrossRef](#)]
16. Liu, S.S.; Ye, M.Q.; Han, A.J.; Chen, X. Preparation and characterization of energetic materials coated superfine aluminum particles. *Appl. Surf. Sci.* **2014**, *288*, 349–355. [[CrossRef](#)]
17. Dai, J.; Xu, J.B.; Wang, F.; Tai, Y.; Shen, Y.; Shen, R.Q.; Ye, Y.H. Facile formation of nitrocellulose-coated Al/Bi<sub>2</sub>O<sub>3</sub> nanothermites with excellent energy output and improved electrostatic discharge safety. *Mater. Des.* **2018**, *143*, 93–103. [[CrossRef](#)]
18. Jiang, H.Y.; Yu, J.; Wang, X.J.; Jiao, X.Y.; Mu, X.G. Preparation, Characterization and Properties of NC-coated Zirconium Composite Particles. *J. Phys. Conf. Ser.* **2023**, *2478*, 032063. [[CrossRef](#)]
19. Tisdale, J.T.; Hill, L.G.; Duque, A.L. Production of desensitized, ultrafine PETN powder. *Powder Technol.* **2022**, *396*, 152–157. [[CrossRef](#)]
20. Xu, C.; Liu, M.Y.; Ma, J.J.; Hou, C.H. Effect of magnesium sulfate heptahydrate micro-encapsulated on HMX safety performance. *J. Ordnance Equip. Eng.* **2022**, *43*, 6.
21. Song, Y.L.; Huang, Q.; Jin, B.; Peng, R.F. Electrostatic self-assembly desensitization of CL-20 by enhanced interface interaction. *J. Alloys Compd.* **2022**, *900*, 163504. [[CrossRef](#)]
22. Zhang, W.P.; Huang, Y.F.; Du, J.F.; Guo, H.L. Research on influencing mechanical sensitivity of dihydroxylammonium 5,5'-bistetrazole-1,1'-diolate(HATO). *Appl. Chem. Ind.* **2022**, *51*, 706–709.
23. Phillips, J.J.; Ching, M.L. A comparative study of two BAM designs for friction sensitivity testing of explosives. *Propellants Explos. Pyrotech.* **2020**, *45*, 628–636. [[CrossRef](#)]
24. Chang, S.J.; Xu, J.J.; Chen, S.L.; Luo, X.C.; Zhang, Z.G.; Bai, J. Approach to the force characterization of the friction sensitivity of the insensitive single explosives. *J. Saf. Environ.* **2020**, *20*, 2218–2222.
25. Song, Y.L.; Huang, Q.; Zhang, J.H.; Zhang, Y.J.; Jin, B.; Peng, R.F. Interaction-Enhanced Coating of Energetic Material: A Generally Applicable Method for the Desensitization. *Propellants Explos. Pyrotech.* **2022**, *47*, e202100256. [[CrossRef](#)]
26. Qin, Y.; Yuan, J.M.; Sun, H.; Liu, Y.; Zhou, H.P.; Wu, R.Q.; Chen, J.F.; Li, X.X. Experiment and Molecular Dynamic Simulation on Performance of 3, 4-Bis (3-nitrofurazan-4-yl) furoxan (DNTF) Crystals Coated with Energetic Binder GAP. *Crystals* **2023**, *13*, 327. [[CrossRef](#)]
27. Gao, J.; Wang, H.; Luo, Y.M.; Wang, H.X.; Wang, W. Study on binary phase diagram of DNAN/DNMF mixed system and its mechanical sensitivity. *Chin. J. Explos. Propellants* **2020**, *43*, 213–218.
28. Kou, Y.; Song, X.L.; Guo, K.G.; Wang, Y. New Method to Prepare the Lowest Eutectic Mixture of MTNP/DNMF and Its Properties. *Combust. Explos. Shock. Waves* **2022**, *58*, 68–76. [[CrossRef](#)]
29. Xiao, C.; Yu, Q.; Zheng, X.Y.; Zheng, B.H.; Guo, Y.; Luo, G.; Jin, B.; Li, J.S. High-Performance and Insensitive DNMF-DFTNAN Eutectic: Binary Phase Diagram and Characterization. *Propellants Explos. Pyrotech.* **2022**, *47*, e202200166. [[CrossRef](#)]
30. Yu, Z.H.; Song, X.L.; Kou, Y.; Wang, Y.; An, C.W. Characterization and Testing for Lowest Eutectic Mixture of TNBA/DNMF. *Propellants Explos. Pyrotech.* **2023**, *48*, e202200201. [[CrossRef](#)]
31. Wang, H.; Gao, J.; Tao, J.; Luo, Y.M.; Jiang, Q.L. Safety and molecular dynamics simulations of DNMF/HATO hybrid systems. *Chin. J. Energetic Mater.* **2019**, *27*, 897–901.

32. Xiao, J.J.; Wang, W.R.; Chen, J.; Ji, G.F.; Zhu, W.; Xiao, H.M. Study on structure, sensitivity and mechanical properties of HMX and HMX-based PBXs with molecular dynamics simulation. *Comput. Theor. Chem.* **2012**, *999*, 21–27. [[CrossRef](#)]
33. Eslami, H.; Khanjari, N.; Müller-Plathe, F. A local order parameter-based method for simulation of free energy barriers in crystal nucleation. *J. Chem. Theory Comput.* **2017**, *13*, 1307–1316. [[CrossRef](#)] [[PubMed](#)]
34. Ma, S.; Li, Y.J.; Li, Y.; Luo, Y.J. Research on structures, mechanical properties, and mechanical responses of TKX-50 and TKX-50 based PBX with molecular dynamics. *J. Mol. Model.* **2016**, *22*, 1–11. [[CrossRef](#)]
35. Weiner, J.H. Statistical Mechanics of Elasticity. *J. Appl. Mech.* **1984**, *51*, 707–708. [[CrossRef](#)]
36. Xiao, J.J.; Huang, Y.C.; Hu, Y.J.; Xiao, H.M. Molecular dynamics simulation of mechanical properties of TATB/fluorine-polymer PBXs along different surfaces. *Sci. China Ser. B Chem.* **2005**, *48*, 504–510. [[CrossRef](#)]
37. Wang, K.; Li, H.; Li, J.Q.; Xu, H.X.; Zhang, C.; Lu, Y.Y.; Fan, X.Z.; Pang, W.Q. Molecular dynamic simulation of performance of modified BAMO/AMMO copolymers and their effects on mechanical properties of energetic materials. *Sci. Rep.* **2020**, *10*, 18140. [[CrossRef](#)]
38. Xin, D.R.; Han, Q. Study on thermomechanical properties of cross-linked epoxy resin. *Mol. Simul.* **2015**, *41*, 1081–1085. [[CrossRef](#)]
39. Hu, Y.Y.; Chen, C.Y.; Chen, K. Molecular Dynamics Simulation of Mechanical Properties of Single-base and Double-base Propellants. *J. Nanjing Xiaozhuang Univ.* **2007**, *23*, 47–50.
40. Ma, Y.X.; Liu, C.; Wang, H.; Zhang, G.X.; Chen, H.; Zhang, W.B. Mechanical Property of the Single TATB Granule by Uniaxial Compression. *Chin. J. Energetic Mater.* **2020**, *28*, 960–968.

**Disclaimer/Publisher’s Note:** The statements, opinions and data contained in all publications are solely those of the individual author(s) and contributor(s) and not of MDPI and/or the editor(s). MDPI and/or the editor(s) disclaim responsibility for any injury to people or property resulting from any ideas, methods, instructions or products referred to in the content.